Available online at www.sciencedirect.com
SCIENCE DIRECT®
Bioelectrochemistry 60 (2003) 37–45
Bioelectrochemistry
www.elsevier.com/locate/bioelechem

Electrochemical study on the keto-enol tautomerization of *p*-hydroxyphenylpyruvic acid in aqueous solution

Yuwu Chi[a], Jianping Duan[b], Xiuzhen Qi[a], Guonan Chen[a,*]

[a] *Department of Chemistry, Fuzhou University, Fuzhou, Fujian 350002, China*
[b] *Analytical and Testing Center, Fuzhou University, Fuzhou, Fujian 350002, China*

Received 18 December 2002; received in revised form 18 March 2003; accepted 25 March 2003

Abstract

The keto-enol tautomerization of *p*-hydroxyphenylpyruvic acid (*p*HPP) in aqueous solutions and the complexation reaction between enolic *p*HPP and boric acid have been studied by electrochemical techniques including linear sweep voltammetry (LSV), pulse voltammetry, and cyclic voltammetry (CV), combining with UV spectrometry. Electrochemical techniques reveal that in aqueous solution, there are two tautomers of *p*HPP: enolic form and ketonic form; the former exists mainly in freshly prepared *p*HPP solution, and the latter exists mainly in equilibrium solution. Both enolic and ketonic *p*HPP are electroactive. The electrochemical oxidation of enolic *p*HPP gives rise to two anodic waves, I_a and II_a, while the electrochemical oxidation of ketonic *p*HPP only results in the observation of the second wave II_a. The oxidation process I_a is revealed to be associated with the quasi-reversible, two-electron two-proton oxidation of "C=C"group at the side chain of enolic *p*HPP, and the oxidation process II_a is proposed to result from the irreversible oxidation of phenolic hydroxyl group. It is observed that in aqueous solution, enolic *p*HPP can quickly complex with boric acid to yield enol-borate complex that can also oxidize at a glassy carbon electrode to yield an anodic wave.

Keywords: Keto-enol tautomerization of *p*-hydroxyphenylpyruvic acid; Electrochemistry

1. Introduction

p-Hydroxyphenylpyruvic acid (*p*HPP) is an important intermediate in the metabolism of tyrosine. Under normal circumstances, *p*HPP is readily converted to 2,5-dihydroxyphenylacetic acid by *p*-hydroxyphenylpyruvate oxidase and the levels of *p*HPP encountered in blood and urine are extremely low. However, in a few individuals suffering from a congenital metabolic defect known as tyrosinemia, the oxidase is not available which leads to dramatic elevation of *p*HPP levels in blood and urine [1]. Because of its biological and clinical significance, chemical reactions of *p*HPP have been studied quite extensively. Among these reactions, the most interesting is the tautomerization of *p*HPP from enolic (**I**) to ketonic (**II**) form (Scheme 1) in aqueous solutions. This kind of reaction has been recognized and studied by following the increased solubility, decreased ultraviolet absorption, and increased reaction with phenylhydrazine. Although the electrochemical behavior of tyrosine and its metabolites has been studied widely[2–5], no attention has been paid to the electrochemical behavior of *p*HPP. Therefore, this paper will focus the study on the electrochemical behaviors of enolic *p*HPP, ketonic *p*HPP and enol-borate complex, and on the enol–keto tautomerization and complexation between enolic *p*HPP and boric acid using electrochemical methods.

2. Experimental

2.1. Chemicals

p-Hydroxyphenylpyruvic acid (*p*HPP) was obtained from Sigma (USA). Other chemicals were of analytical grade and used as supplied by the manufacturer.

Stock solutions of *p*HPP (1×10^{-2} mol/l) were prepared by dissolving the required amount of sample in methanol and stored under refrigeration in an amber bottle. Normally

* Corresponding author. Tel.: +86-591-7893315; fax: +86-591-3713866.
E-mail address: gnchen@fzu.edu.cn (G. Chen).

1567-5394/03/$ - see front matter © 2003 Elsevier Science B.V. All rights reserved.
doi:10.1016/S1567-5394(03)00044-6

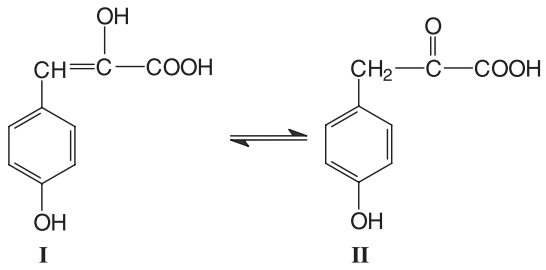

Scheme 1.

the aqueous solution contains more dissolved oxygen than methanol, so *p*HPP, which is easily oxidized by oxygen, is stable in methanol but unstable in aqueous solution. Therefore, aqueous solutions of *p*HPP for testing were prepared by injecting an accurate volume of concentrated *p*HPP solution into the electrochemical cell containing the appropriate buffer (pH 2–12), which had been degassed for 10 min with high purity nitrogen to remove oxygen. The solution was examined immediately, during which a continuous stream of nitrogen was passed over the solution.

The buffer system was a phosphate buffer (pH 2–12.0) prepared by titrating a stock solution containing 0.1 mol/l phosphate acid with sodium hydroxide to the desired pH value.

2.2. Apparatus

A Microcomputer-based Electrochemical Analyzer (Tianjin Lanlike, China) was employed for linear voltammetric and cyclic voltammetric measurements with a glassy carbon electrode (GCE, Princeton Applied Research, Princeton, NJ) having an approximate area of 7 mm^2. A BAS-100A Electrochemical Analyzer (Bioanalytical Systems, Purdue, IN, USA) was used for double-step chronocoulometric, pulse voltammetric measurements with a GCE. All potentials were measured against an Ag/AgCl (3 mol/l KCl) reference electrode. The parameters used for the measurements were as the follows:

(a) Linear sweep and cyclic voltammetry (CV): scan rate 200 mV/s.
(b) Differential pulse voltammetry (DPV): pulse period 1 s, pulse amplitude 50 mV, pulse width 20 ms.

Ultraviolet absorption spectra were recorded on a Lambda 9 spectrophotometer (Perkin-Elmer).

3. Results and discussion

3.1. Keto-enol tautomerization of pHPP in aqueous solution

It was found that enolic form of *p*HPP remained very stable in methanol medium, i.e. its UV spectrum (λ_{max} = 219 nm, $\varepsilon_{219\ nm}$ = 22,000) would not change in 1 month after the *p*HPP crystal (existing in enolic form) has been dissolved. However, the enolic form of *p*HPP would be converted to the ketonic form in aqueous solution, which is so-called tautomerization. This tautomerization reaction is recognized to be spontaneous and can be followed by UV spectroscopy. Fig. 1 shows clearly the UV spectrum of *p*HPP (1×10^{-4} mol l^{-1}) change with time after the stock enolic *p*HPP methanol solution (1×10^{-2} mol l^{-1}) has been diluted with double-distilled water. Curve a in Fig. 1 is the UV spectrum recorded as soon as the enolic *p*HPP was diluted with water. This UV spectrum is the same as that of enolic *p*HPP in methanol medium with the characteristic bands (λ_{max} = 219 nm, $\varepsilon_{219\ nm}$ = 22,000), which indicates that almost all *p*HPP molecules still exist in enolic form shortly after the *p*HPP aqueous solution has been prepared. Then, the spectrophotometric adsorption at λ_{max} 291 nm was observed to decrease slowly with time (Curves b–m in Fig. 1). In the meantime, a new spectrophotometric adsorption associated with ketonic *p*HPP appears at λ_{max} 280 nm. It is also evident from Fig. 1 that the molar absorptivity value of ketonic *p*HPP at λ_{max} 280 nm ($\varepsilon_{238\ nm}$ = 3500) is much smaller than that of enolic *p*HPP at λ_{max} 291 nm ($\varepsilon_{291\ nm}$ = 22,000). Furthermore, their absorption peaks are very closely spaced ($\Delta\lambda_{max}$ = 11 nm). Thus, the absorption peak of ketonic *p*HPP is completely merged with that of enolic *p*HPP and cannot be observed until the solution of *p*HPP on 7 h standing (see Curve h in Fig. 1). Finally, the keto-enol tautomerization equilibrium is reached after 24 h (see Curve m in Fig. 1). It is apparent that most *p*HPP molecules exist in ketonic form whereas only a few *p*HPP molecules exist in enolic form in the equilibrium solution.

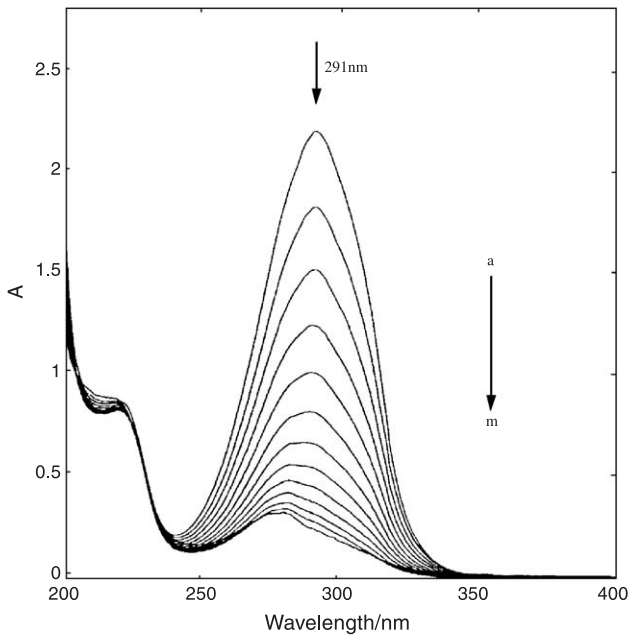

Fig. 1. The variation of UV spectrum of *p*HPP (1×10^{-4} mol l^{-1} in double distilled water) with time: (a) 0, (b) 1, (c) 2, (d) 3, (e) 4, (f) 5, (g) 6, (h) 7, (i) 8, (j) 9, (k)10, (l) 11, (m) 24 h.

3.2. Electrochemical behavior of tautomers of pHPP in the absence of boric acid

Although the mutual influence was not found between enolic and ketonic forms of *p*HPP when they coexist in the solution, to avoid the mutual influence during the investigation of electrochemical behavior of tautomers of *p*HPP, we can study the electrochemical behaviors of enolic and ketonic forms of *p*HPP independently by controlling some experimental conditions. On one hand, in order to investigate the electrochemical behavior of the enolic form of *p*HPP without the interference of the ketonic form, the stock solution of *p*HPP was injected into desired buffer solution (not containing boric acid), which had been degassed for 10 min, then the test solution was stirred and measured as quickly as possible. On the other hand, to investigate the electrochemical behavior of ketonic form of *p*HPP with the minimum interference of enolic form of *p*HPP, the electrochemical measurements were carried out after the tautomerization equilibria were reached (after 24 h.).

3.2.1. Linear sweep voltammetry (LSV)

The linear sweep voltammograms of freshly prepared solution of *p*HPP (largely in enolic form) and equlibrium solution of *p*HPP (largely in ketonic form) at the GCE over a range of pH values are shown in Fig. 2A and B, respectively. These LSV curves show clearly that the electrochemical behaviors of enolic and ketonic *p*HPP are quite different.

3.2.1.1. Enolic pHPP. Fig. 2A shows that oxidation of enolic *p*HPP gives rise to two anodic waves. The first oxidation wave (I_a) occurs at relatively low potential and exists in the phosphate buffer solution over the pH range 2 to 10.0 (see Curve a–i in Fig. 2A). In strongly acidic media (pH 2.0–4.0), I_a is much higher and sharper than in other media. This indicates that I_a has the characteristics of reactant adsorption in strongly acidic media. The peak current of I_a of enolic *p*HPP does not change over the pH range 2.0 to 4.0 (Fig. 2A, a–c). However, I_a decreases sharply with increasing pH over the pH range 4.0 to 5.0 (Fig. 2A, c–d). Then, I_a decreases slowly with increasing pH over the pH range 5.0 to 10.0 (Fig. 2A, d–i). Finally, I_a disappears when pH is higher than 10.0. The second oxidation wave (II_a) of enolic *p*HPP is found at a more positive potential and exists in the buffer over the pH range 2 to 12.0 (see Curves a–k in Fig. 2A). Unlike I_a, the peak current of II_a decreases slowly over the whole pH range examined. The variations of peak potentials of I_a and II_a with pH are shown in Table 1. Both the peak potentials of I_a and II_a shift to more negative potential as the pH is increased, which indicates that one or more protons are possibly involved in these two oxidation processes of enolic *p*HPP. In terms of molecular structure of enolic *p*HPP, the anodic waves I_a and II_a can be considered to be associated with oxidation of "C=C" group at the side chain and phenolic hydroxyl group, respectively. Actually, it is found that electrochemical behavior of the second oxidation process (II_a) of enolic *p*HPP is very similar to that of its metabolic precursor tyrosine [6] by comparing their LSV

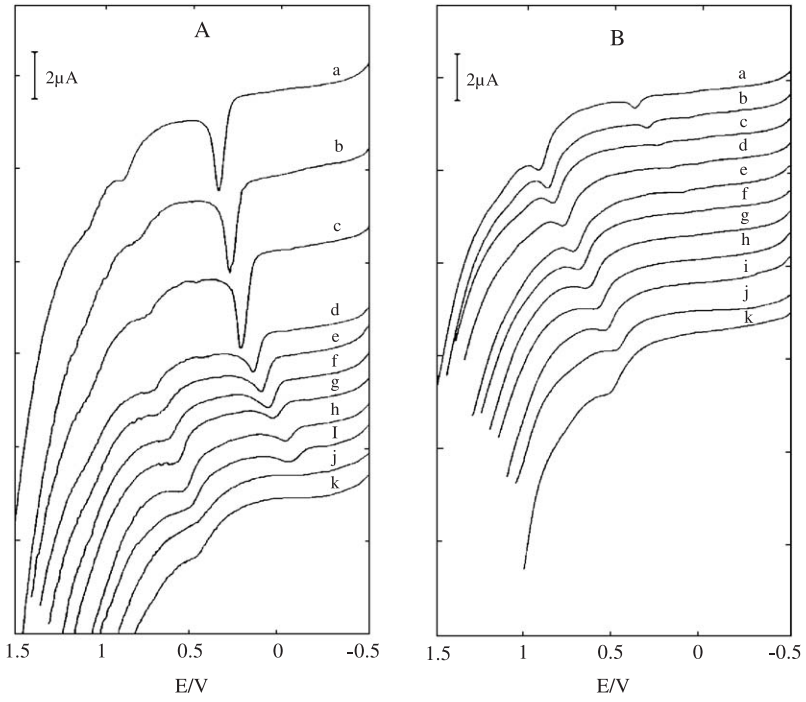

Fig. 2. Linear sweep voltammograms obtained at the GCE for freshly prepared *p*HPP solution (A) and equilibrium *p*HPP solution (B) in 0.1 mol l^{-1} phosphate buffer at pH: (a) 2.0, (b) 3.0, (c) 4.0, (d) 5.0, (e) 6.0, (f) 7.0, (g) 8.0, (h) 9.0, (i) 10.0, (j) 11.0, (k) 12.0.

Table 1
Dependence of LSV peak potentials of *p*HPP (vs. Ag/AgCl) on pH

Process	Enolic *p*HPP	Ketonic *p*HPP
I_a	$E_{Ia\ (pH2.0-10.0)}$= (0.430−0.054 pH) V	
II_a	$E_{IIa\ (pH2.0-11.0)}$= (0.965−0.048 pH) V	$E_{IIa\ (pH2.0-11.0)}$= (1.026−0.048 pH) V
	$E_{IIa\ (pH>11.0)}$ = 0.450 V	$E_{IIa\ (pH>11.0)}$ = 0.498 V

curves. This suggests that II_a is associated with the electrochemical oxidation of phenolic hydroxyl group, which is known to be an irreversible one-electron process. Unlike the oxidation of phenolic hydroxyl group, the oxidation of side chain "C=C" group has very low oxidation potentials in alkaline media, e.g. the E_{Ia} at pH 10 is about −0.110 mV (vs. Ag/AgCl). This suggests that the side chain of enolic *p*HPP be very easily oxidized by dissolved oxygen in the alkaline solution. Actually, this kind of chemical oxidation of *p*HPP in alkaline solution has been investigated and suggested to produce *p*-hydroxybenzaldehyde and oxalate. Because I_a, as described previously, has a better define peak shape and relative high oxidation potential in strongly acidic solution (pH 2.0–4.0) than in the other buffer solution, pH 2.0 phosphate buffer is selected for the subsequence experiments.

At various scan rates, LSV measurements were carried out for enolic *p*HPP in pH 2.0 phosphate buffer solution. The effect of scan rate on the oxidation peak potential is shown in Table 2. It can be known from Table 2 that both E_{Ia} and E_{IIa} shift to more positive potentials with increasing scan rate, indicating that both I_a and II_a oxidation processes are irreversible or quasi-reversible. The effect of scan rate on the oxidation peak currents is shown in Fig. 3. For oxidation process I_a, the peak current (i_{Ia}) is proportional to scan rate, v, over the range of 5–200 mVs^{-1} (see Fig. 3A), indicating that the electrode process is adsorption-controlled at low scan rate. However, i_{Ia} becomes proportional to $v^{1/2}$ over the scan rate range of 200–1000 mVs^{-1} (see Fig. 3B), which indicates that the electrode process is diffusion-controlled at fast scan rates. For the oxidation process II_a, the peak current (i_{IIa}) increases linearly with $v^{1/2}$ over the range of 5–800 mVs^{-1} (see Fig. 3B), indicating that at the peak potentials the electrode process is diffusion-controlled at the examined scan rates[7].

3.2.1.2. Ketonic pHPP. The LSV curves of equilibrium solutions of *p*HPP at various pH are shown in Fig. 2B. In equilibrium solution, process I_a, corresponding to the oxidation of "C=C" group at the side chain of enolic *p*HPP, tends to disappear by comparing with the case of freshly prepared solution (Fig. 2A). I_a can be seen with quite small peak current in acidic solutions (Fig. 2B, Curves a–e), but almost disappears in neutral and alkaline media (Fig. 2B, Curves f–k). The change of current of I_a indicates that enolic *p*HPP with electroactive side chain (−CH=C(OH)COOH) converts to ketonic *p*HPP without electroactive side chain (−CH2−COCOOH) during the spontaneous tautomerization. However, unlike the remarkable change of I_a taking place during the tautomerization, II_a of ketonic *p*HPP can be clearly observed at all examined pH range (Fig. 2B, Curves a–k); the variation of peak potential of II_a of ketonic *p*HPP with pH is also shown in Table 1. The very similar LSV responses of II_a suggest that II_a processes of ketonic and enolic *p*HPP involve the same oxidation mechanism, i.e. II_a processes are associated with the oxidation of phenolic hydroxyl group. As has been described above, at pH 7.0 or higher, enolic *p*HPP is basically changed to ketonic *p*HPP, but it is found that if pH is too high (>10.0), ketonic *p*HPP becomes unstable in aqueous solution. So pH 7.0 is selected for further electrochemical study of ketonic *p*HPP.

At various scan rates, LSV measurements were carried out for ketonic *p*HPP in pH 7.0 phosphate buffer solution. The effect of scan rate on the oxidation peak potential of II_a is shown in Table 3. It can be known from Table 3 that the oxidation peak potential of II_a shifts to more positive potential with increasing scan rate, which indicates that the oxidation process of ketonic *p*HPP is irreversible. The effect of scan rate on the oxidation peak current is shown in Fig. 4. It can be found that the peak current of II_a for ketonic *p*HPP is not proportional to scan rate v (see Fig. 4A), but proportional to $v^{1/2}$ (see Fig. 4B) over the range of 5–1000 mVs^{-1}. This suggests that the electrode process II_a for ketonic *p*HPP is diffusion-controlled at the examined scan rates [7].

3.2.2. Differential pulse voltammetry (DPV)

By comparing the LSV peak currents of I_a of enolic *p*HPP shown in Fig. 2A with those of equilibrium solution shown in Fig. 2B, the apparent distribution coefficients of enolic *p*HPP and ketonic *p*HPP might have been calculated. However, in order to obtain more precise results, DPV was employed. The apparent distribution coefficients of enolic and ketonic *p*HPP obtained from the DPV measurement are shown in Fig. 5. It clearly indicates that in strongly acidic media, there are still quite a few *p*HPP molecules that exist in enolic form; for example, the apparent distribution coefficient of enolic form is about 0.28 at pH 2.0. But almost all of *p*HPP molecules exist in ketonic form when pH value is higher than 6; for example, at pH 7, the apparent distribution coefficient of ketonic form is larger than 0.99. Thus, pH 7.0 sodium phosphate was adopted for further investigation of ketonic *p*HPP.

Table 2
LSV peak potentials of enolic *p*HPP at various scan rates

v (mVs^{-1})	5	10	20	50	100	200	400	600	800	1000
E_{Ia} (mV)	392	392	396	399	400	402	409	408	412	414
E_{IIa} (mV)	927	930	932	950	950	959	961	971	972	

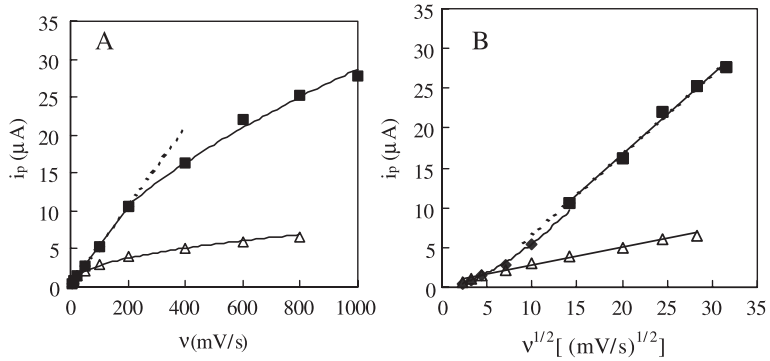

Fig. 3. Influence of scan rate on the LSV peak current for oxidation of 1×10^{-4} mol l^{-1} enolic *p*HPP at a GCE for processes I_a (■) and II_a (△) in pH 2.0 phosphate buffer. (A) Plot of peak current (i_p) vs. scan rate (v). (B) Plot of peak current (i_p) vs. square root of scan rate ($v^{1/2}$).

3.2.3. Cyclic voltammetry (CV)

3.2.3.1. Enolic pHPP. In order to further reveal the mechanism of electrochemical oxidation of enolic *p*HPP at the GCE, the CV measurements were carried out for freshly prepared solutions of enolic *p*HPP in pH 2.0 phosphate buffer. Fig. 6A shows the cyclic voltammogram of enolic *p*HPP at a GCE over the potential range −500 to +1500 mV. On the first sweep to positive potentials appear two oxidation peaks (I_a and II_a) corresponding to oxidation processes I_a and II_a, respectively. On the reverse sweep, a reduction peak I_c appears at the potential about 30 mV more negative than the potential of I_a. Peaks I_c and I_a seem to form a quasi-reversible couple because the peak current of I_a is much higher than that of I_c. Unlike the case with I_a, there is no reduction peak coupled to oxidation peak II_a in the reverse potential scan. These indicate that oxidation process I_a is quasi-reversible whereas oxidation process II_a is totally irreversible. On the subsequent sweeps, the peak currents of both I_a and II_a are decreased rapidly, suggesting that these oxidation processes produce some strongly adsorbed species and result in deactivation of the electrode surface. Simultaneously, a new quasi-reversible redox couple (I_a' and I_c') appears and increases with increasing sweep cycles. It is interesting that when the tested electrode is subsequently washed and placed in buffer again, peaks I_a, II_a, and I_c disappear whereas peak heights of the new redox couple (I_a' and I_c') keep unchanged for several hours (figure not shown here). This indicates that oxidation proceeds via an ECE mechanism, i.e. the oxidation of *p*HPP is followed by a rapid chemical step, resulting in the generation of a strongly adsorbed and electroactive species at the surface of GCE. In order to reveal the relationship between the subsequently formed redox couple (I_a'/I_c') and the two original oxidation peaks I_a and II_a, the CV experiment was undertaken over the potential range −500 to +700 mV, where only the oxidation of side chain of enolic *p*HPP (process I_a) occurs but no reaction associated with the oxidation of phenol group (II_a) of enolic *p*HPP can happen. Under the above potential condition, the cyclic voltammogram obtained for enolic *p*HPP (Fig. 6B) shows that the subsequently formed redox couple (I_a'/I_c') described above (see Fig. 6A) cannot be observed in the absence of second oxidation process II_a. It means that this new redox couple is due to the oxidation of phenol group (process II_a) followed by a rapid chemical reaction and formation of a strongly adsorbed electroactive species. These kinds of ECE oxidation reactions have also been reported for phenol derivatives such as methoxyphenols and tyrosine [3], and the oxidation mechanism has been suggested as that the one-electron process yields dimers that react to form dimeric quinones and polymers. Thus, it can follow that the redox couple (I_a'/I_c') observed in the oxidation of *p*HPP is due to the subsequent formation of dimeric quinones. This conclusion is also supported by the fact that electrochemical behaviors of the redox couple (I_a'/I_c') are very similar to that of benzoquinone except that the former is strongly adsorbed at the surface of the GCE, whereas the latter is not at all adsorbed at the electrode. Additionally, Fig. 5B shows more clearly compared with Fig. 5A that peak I_a and I_c indeed form a quasi-reversible redox couple. The redox couple is centered at +400 mV with a ΔE_{peak} of 30 mV.

Table 3
LSV peak potentials of ketonic *p*HPP at various scan rates

v (mVs^{-1})	5	10	20	50	100	200	400	600	800	1000
E_{IIa} (mV)	685	691	697	708	714	723	730	737	746	757

3.2.3.2. Ketonic pHPP. The cyclic voltammetric measurement was carried out for ketonic *p*HPP(1.0×10^{-4} mol l^{-1}) in pH 7.0 phosphate medium. Except that I_a/I_c redox couple is not observed for ketonic *p*HPP, the cyclic voltammogram of ketonic *p*HPP shown in Fig. 7 is very similar to that of enolic *p*HPP shown in Fig. 6A. This indicates that an ECE mechanism is also involved in the oxidation of ketonic *p*HPP as the case of enolic *p*HPP described above, i.e. an irreversible oxidation of phenol group of ketonic *p*HPP (II_a) is followed by a rapid chemical step, resulting in the generation of a strongly adsorbed and electroactive species; then these species can be further oxidized giving rise to a quasi-reversible oxidation process (I_a').

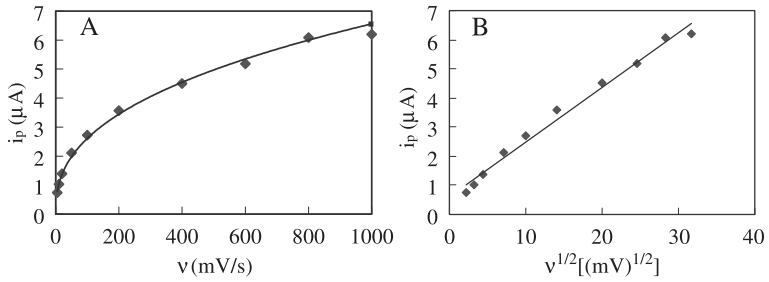

Fig. 4. Influence of scan rate on the LSV peak current for oxidation of 1×10^{-4} mol l^{-1} ketonic *p*HPP at a GCE for process II_a in pH 7.0 phosphate buffer. (A) Plot of peak current (i_p) vs. scan rate (v). (B) Plot of peak current (i_p) vs. square root of scan rate ($v^{1/2}$).

3.3. The electrochemical behaviors of pHPP in the presence of boric acid

It was found that the electrochemical behavior of enolic *p*HPP in the presence of boric acid differed from that in the absence of boric acid. In phosphate buffer (not containing boric acid), as described above, the oxidation of the "C=C" group at the side chain of enolic *p*HPP gave rise to a single oxidation wave, I_a, over a wide pH range (pH2.0–10.0). However, in Britton–Robinson buffer, which contains 0.04 mol l^{-1} boric acid, when pH was 3.0 or higher (3.0–10.0), the single oxidation wave cleaved into two waves, the original wave I_a and a new wave III_a. Evidently, the former is associated with oxidation of enolic *p*HPP itself, the latter is associated with oxidation of a new compound resulted from the reaction of enolic *p*HPP with boric acid. It has been confirmed with UV spectroscopy that boric acid could react with the enolic *p*HPP to form an enol-borate. This reaction shown in Scheme 2 is very analogous to the well-known reaction of boric acid with ethylene glycol, i.e. two molecules of enolic *p*HPP react with one molecule of boric acid to form a new complex (**III**). In strongly acidic media (pH 3.0), III_a was rather small, but III_a was increased and reached to a constant value when pH was higher than 4.0. It is evident that the dependence of peak current of III_a on pH results from that the complexation reaction of enolic *p*HPP with boric acid involving splitting off one proton. So, at a certain pH range (pH 2.0–5.0), the higher is the pH, the more complex are the molecules produced. Similar to the case for I_a, the peak potential of III_a also shifts to more negative potential with increasing pH, which indicates that the oxidation of enol-borate complex involves proton transfer. Paralleling with variation of peak current of III_a with pH, peak current of I_a decreased with pH and reached a constant value; however, the total oxidation current of I_a and III_a was equal to the oxidation current of I_a for the case where no boric acid existed in the buffer. In order to reveal the mechanism of the complexation reaction of enolic *p*HPP with boric acid, the effect of the concentration of boric acid on the complexation equilibrium was investigated. In this experiment, acetate buffer (pH 4.5) was selected and various amounts of boric acid (form 0 to 0.2 mol l^{-1}) were added to enolic *p*HPP

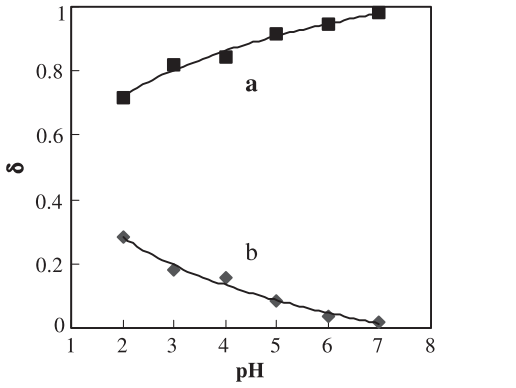

Fig. 5. The distribution curves of ketonic *p*HPP (a) enolic *p*HPP (b) in various pH equilibrium solutions obtained by differential pulse voltammetry.

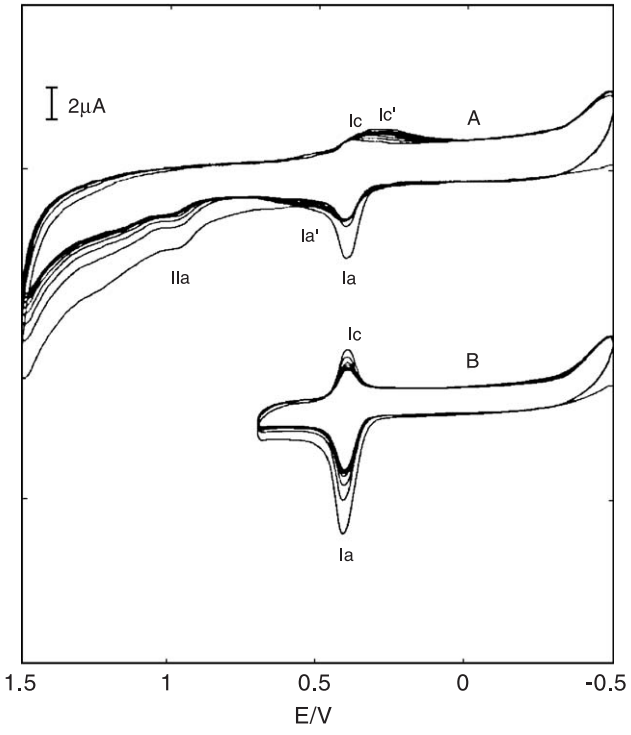

Fig. 6. Cyclic voltammograms obtain at the GCE for 1×10^{-4} mol l^{-1} enolic *p*HPP in pH 2.0 phosphate buffer with sweep segments: 20, scan rate: 200 mV s^{-1}, initial potential: −0.500 V, and final potentials: (A) 1.500 V, (B) 0.700 V vs. Ag/AgCl.

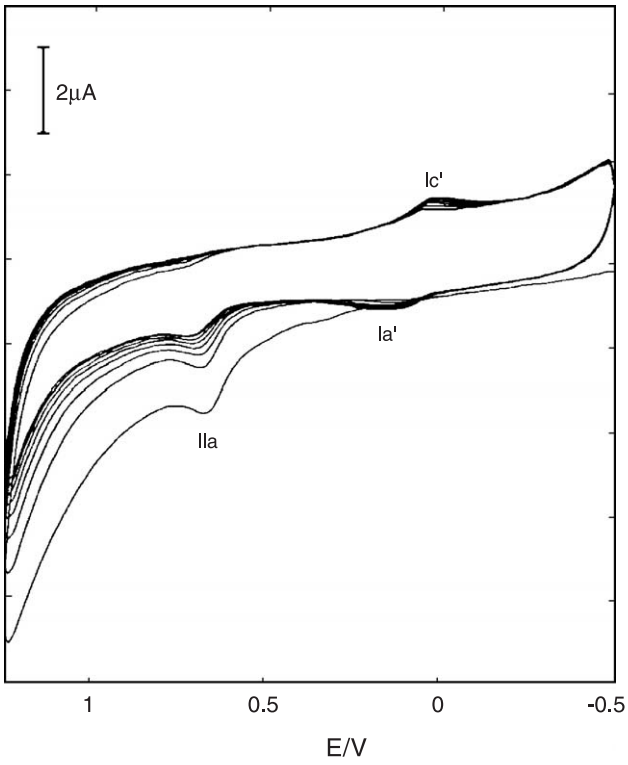

Fig. 7. Cyclic voltammograms obtain at the GCE for 1×10^{-4} mol l^{-1} ketonic *p*HPP in pH 2.0 phosphate buffer with sweep segments: 20, scan rate: 200 mV s^{-1}.

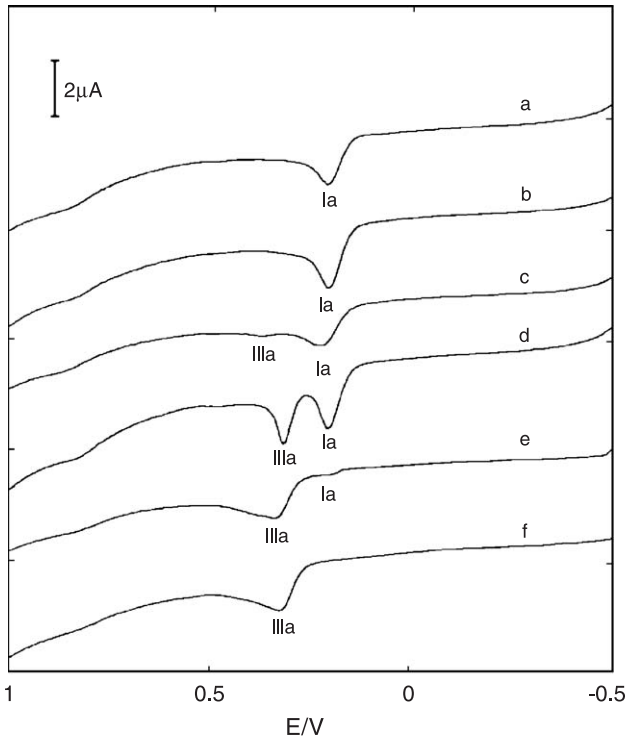

Fig. 8. Linear sweep voltammograms obtained at GCE for 1×10^{-4} mol l^{-1} enolic *p*HPP in pH 4.5 acetate buffer in the presence of boric acid of various concentrations: (a) 0, (b) 1×10^{-4}, (c) 1×10^{-3}, (d) 1×10^{-2}, (e) 0.1, and (f) 0.2 mol l^{-1}.

solution. The results are shown in Fig. 7. When the concentration of boric acid is at the range of $0-1.0 \times 10^{-4}$ mol l^{-1}, only I_a corresponding to enolic *p*HPP is observed (Fig. 8, Curves a–b), which means that the formation of complex compound, enol-borate, may be neglected at low concentration of boric acid. But as the concentration of boric acid increases, III_a corresponding to enol-borate begins to appear (Fig. 8, Curve c) and increases until a constant value is reached (Fig. 8, Curves d–f). Simultaneously, I_a corresponding to the oxidation of enolic *p*HPP decreases (Fig. 8, Curves d–e) and disappears completely when the concentration of boric acid reaches to 0.2 mol l^{-1}. This means that enolic *p*HPP is almost completely present as the borate complex at high concentration of boric acid. Fig. 8 also shows clearly that although the peak currents of I_a and III_a are both dependent on the concentration of boric acid, their total peak currents do not vary with the concentration of boric acid at all. This indicates that the oxidation of complex (III_a) occurs at enolic *p*HPP rather than at boric acid. The fact that the peak current of I_a at low concentration of boric acid is equal to the peak current of III_a at high concentration of boric acid indicates that both molecules of enolic *p*HPP in enol-borate complex are oxidized during the oxidation of enol-borate complex. According to the tautomerization equilibrium shown in Scheme 2, the equilibrium constant, *K*, can be easily calculated by the data obtained from Fig. 8. For example, Curve d in Fig. 8 shows that peak height of oxidation of enolic *p*HPP (I_a) is equal to that of enol-borate complex (III_a) when the boric acid concentration is 0.01 mol l^{-1}, which means the molecule number of free *p*HPP is

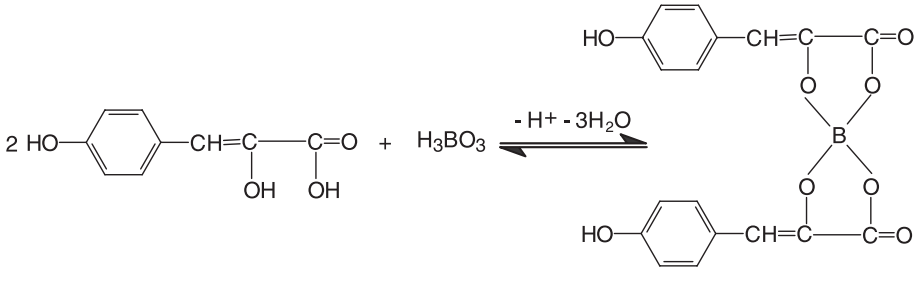

(I) (III)

Scheme 2.

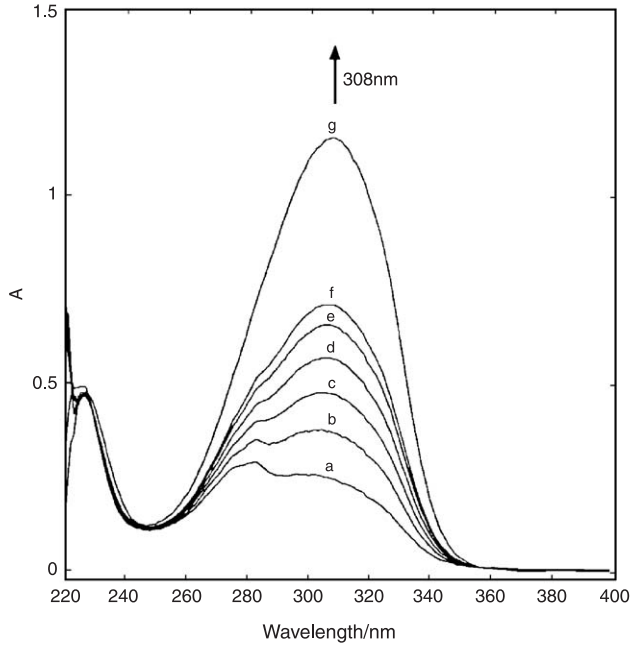

Fig. 9. The variation of UV spectrum of ketonic *p*HPP (1×10^{-4} mol l^{-1} in pH 7.0 phosphate buffer) with time: (a) 1 min, (b) 30 min, (c) 60 min, (d) 90 min, (e) 120 min, (f) 150 min, and (g) 14 h on addition of 0.4 mol l^{-1} boric acid to the ketonic solution.

equal to the molecule number of *p*HPP in enol-borate, so concentrations of enol-borate, free *p*HPP, and free boric acid are 5.0×10^{-5}, 5.0×10^{-5}, and 1.0×10^{-2} mol l^{-1}, respectively. Therefore, the tautomerization equilibrium constant K is calculated to be 1.0×10^{-6} L^2 mol^{-2}, which is close to the value obtained by using UV spectrophotometry.

Additionally, from Fig. 8, it follows that the complexation of enolic *p*HPP with boric acid is far faster than the keto-enol tautomerization because these LSV curves of enolic *p*HPP (Curve a, b), enol-borate complex (Curve f), or their mixture (Curves c–e) could be obtained immediately after the solutions have been prepared. Therefore, based on this conclusion, the reversibility of the tautomerization reaction between enolic and ketonic *p*HPP can be investigated by adding boric acid to the buffer solution. As noted above, the tautomerization reaction from enolic *p*HPP to ketonic *p*HPP is spontaneous in aqueous solution; however, in the presence of boric acid, the reverse process, from ketonic *p*HPP to enolic *p*HPP, has been observed by spectrophotometry. As shown in Fig. 9, upon addition of boric acid, the UV spectra of equilibrium solution (largely ketonic *p*HPP) change with time slowly, i.e. a new absorption at $\lambda_{max} = 308$ nm corresponding to enol-borate complex [6] appears and increases with time (Fig. 9, Curves a–g), and finally reaches a constant value after 14 h (Fig. 9, Curve g). This means, upon addition of boric acid, ketonic *p*HPP changes to enolic *p*HPP slowly, the latter reacts with boric acid quickly giving rise to enol-borate complex; thus, the original tautomerization equilibrium is broken and a new equilibrium involving tautomerization and complexation reaction is established.

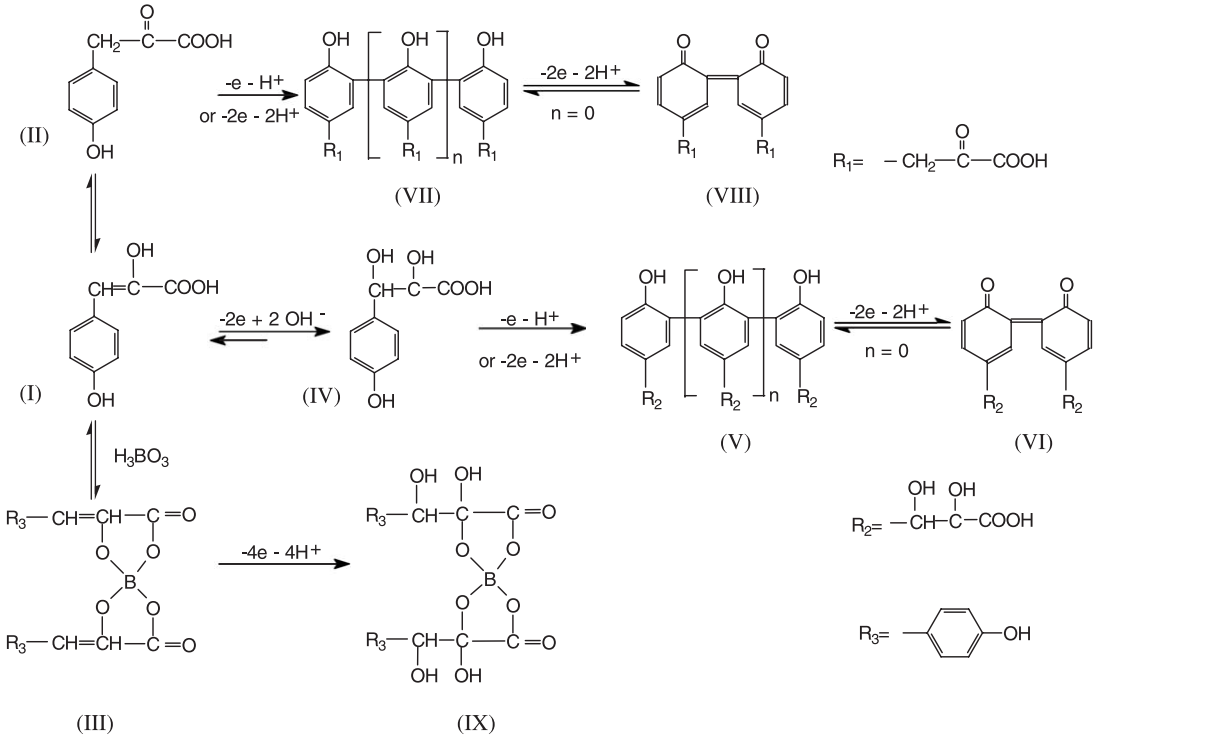

Scheme 3.

3.4. Electrochemical oxidation mechanism of tautomers of pHPP in aqueous solution

In summary, according to the above studies and discussions, Scheme 3 is proposed for the possible tautomerization reaction mechanism of *p*HPP and electrochemical oxidation mechanism of tautomers of *p*HPP at GCE.

*p*HPP has two tautomers, enolic form (**I**) and ketonic form (**II**). In crystal or noaqueous solution, *p*HPP exists largely as enolic *p*HPP, but in aqueous solution, enolic *p*HPP changes spontaneously to ketonic *p*HPP, and exists largely as ketonic *p*HPP in equilibrium solution. The electrochemical oxidation of ketonic *p*HPP gives rise to one single anodic wave II_a, which results from the oxidation of phenolic hydroxyl group via an ECE mechanism. The ECE reaction pathway involves a one- or two-electron transfer followed by a rapid formation of dimer or polymer (**VII**) by coupling free radicals, and subsequent reversible oxidation of **VII** to strongly adsorbed species (**VIII**). The electrochemical oxidation of enolic *p*HPP (**I**) gives rise to two anodic waves. I_a results from the quasi-reversible oxidation of side-chain "C=C" group with two-electron two-proton transfer to yield compound **IV**. II_a is associated with the oxidation of phenolic hydroxyl group of **IV**, which may follow the same ECE pathways involved in the oxidation of ketonic *p*HPP and also yield strongly adsorbed species (**V** and **VI**). In aqueous solution, enolic *p*HPP (**I**) can react reversibly with boric acid to yield enol-borate complex (**III**), which can be irreversibly oxidized to yield the possible product **IX**.

Acknowledgements

This project was financially supported by the National Nature Sciences Funding of China (20175005) and The Science Foundation of State Education Department, China. Yuwu Chi thanks the Science and Technical Development Foundation of Fuzhou University, China (no. XKJ(QD)-0103).

References

[1] C.Y. Zhang, Chinese Medical Encyclopedia, Biochemistry, Shanghai Science and Technology Press, Shanghai, 1987, pp. 245–247.
[2] M.R. Defelippis, C.P. Murthy, F. Broitman, D. Weinraub, M. Faraggi, M.H. Klapper, Gelation of xanthan by trivalent chromic ions monitored by 1H NMR relaxation: a preliminary study, J. Phys. Chem. 95 (1991) 341–344.
[3] S.K. Wheeler, L.A. Coury Jr., W.R. Heineman, Fouling-resistant, polymer-modified graphite electrodes, Anal. Chim. Acta 237 (1990) 141–148.
[4] L.C. Portis, J.T. Klug, C.K. Mann, Electrochemical oxidation of some phenethylamines, J. Org. Chem. 39 (1974) 3488.
[5] D.M. Anjo, K.K. Corkery, E. Gonzalez, K.A. Marantos, K.E. Estrada, Diffusion coefficients of phenolic aromatics by chronocoulometry at the glassy carbon electrode, J. Chem. Eng. Data 39 (1994) 813–816.
[6] A. Hariman, Further comments on the redox potentials of tryptophan and tyrosine, J. Phys. Chem. 91 (1987) 6102–6104.
[7] G.G. Pu, Z.B. Yuan, S.G. Wu, The Electroanalytical Chemistry, Press of Science and Technology University of China, Hefei, 1993, pp. 116–119.